Desalination and Water Treatment
www.deswater.com
doi: 10.5004/dwt.2021.26687

212 (2021) 359–367
February

Zinc oxide porous samples obtained by the sacrifice phase technique as an alternative to water depollution: processing and dye photocatalytic potential

Felipe P. Faria, Thamara M.O. Ruellas, Tania R. Giraldi, Carolina Del Roveri, Sylma C. Maestrelli*

Universidade Federal de Alfenas, Instituto de Ciência e Tecnologia, Rodovia José Aurélio Vilela, 11999, BR 267, KM 533, Cidade Universitária, CEP: 37715-400 Poços de Caldas, MG, Brasil. Brazil, Tel. +55-35-991623224; Mobile No: +55 (35) 36974736; emails: sylma.maestrelli@unifal-mg.edu.br (S.C. Maestrelli), flipfaria@gmail.com (F.P. Faria), thamararuellas@gmail.com (T.M.O. Ruellas), tania.giraldi@unifal-mg.edu.br (T.R. Giraldi), carolina.roveri@unifal-mg.edu.br (C.D. Roveri)

Received 29 June 2020; Accepted 3 October 2020

ABSTRACT

This paper explored the production of porous pieces of ZnO by pressing, with the addition of eucalyptus sawdust as a sacrifice phase to be eliminated after heat treatment to create porosity on the microstructure. The physical properties were measured and the microstructure was evaluated by scanning electron microscopy. The photocatalytic potential of the ZnO pieces and its reuse were evaluated through five cycles of photocatalytic assays. With a compaction pressure of 90 MPa and a 25% weight percentage of eucalyptus sawdust, the samples achieved more than 79% photodegradation. After the fifth cycle, this percentage was around 75%. The results showed that the use of eucalyptus sawdust as a sacrifice phase is an easy and fast processing route to obtain porous ZnO bodies (more than 50% porosity was obtained for all samples), with good photocatalytic results. The porous samples obtained by this technique using eucalyptus sawdust can be a promising alternative to promote the photodegradation of the dyes. The pieces are also chemically inert, easy to handle, providing little loss and possibility of reuse.

Keywords: Sacrifice phase technique; ZnO; Photodegradation of dyes; Rhodamine B; Depollution

1. Introduction

Besides the high consumption of water, textile industrial processes release around 20% of all dye used to color cloth and fibers onto the environment, causing one of the environmental problems of great impact in Brazil, since the sector is cited as one of the eight most important segments in the Brazilian economy [1,2]. Therefore, there are issues such as environmental degradation, depletion of natural resources and final disposal of waste, which leads the academic community to find solutions for these environmental problems.

Significative results for photodegradation based on semiconductors, such as nanometric powders of zinc oxide (ZnO), have been reported as they were applied to systems for effluent decontamination. The high degradation kinetics of the Rhodamine B (RhB) dye has been verified using this semiconductor in photocatalytic processes [2–4]. In these cases, the photoactivation occurs when the incident irradiation on the semiconductors generates hydroxyl radicals, due to redox reactions promoted from species adsorbed on the semiconductor surface, in aqueous medium. These reactions result in the mineralization of the organic compounds [5].

The semiconductors are usually used as suspended particles in a liquid medium, presenting a large surface area and good efficiency in mass transfer processes. Even if some publications indicate the use of these photocatalysts

* Corresponding author.

1944-3994/1944-3986 © 2021 Desalination Publications. All rights reserved.

as nanometric powders, the low practicality of this particular way of management is notorious given that, if the semiconductor powder is not well fixed in a kind of support, the material can be dragged, compromising the effectiveness of the photoactivation and also entail new steps on the treatment [6–8]. Besides, it is difficult to separate semiconductor particles from the reaction medium at the end of the photocatalytic process. The elimination of the separation step of the semiconductors decreases final time of the process and it facilitates the application in an industrial scale. Thus, the conformation of porous powders into ceramic bodies can be the ideal combination between relatively high superficial area, needed in the oxidative process and solving the dragging issue, which is a recurrent problem when using nanometric semiconductor powders. In addition, the production and use of pressed samples also has the advantage that they can be reused in various reaction cycles.

A well-known technique used to produce porous materials consists of incorporating organic compounds inside the ceramic materials [9–11]. This method consists basically of dispersing the organic compounds (denominated sacrifice phase) in the ceramic precursor through the preparation of a homogeneous biphasic mixture in a way that, during the process of sintering, those compounds are eliminated leaving a group of pores with a similar size to the particles initially incorporated.

The product used as a porosity precursor (named sacrifice phase) can be natural or artificial organic materials, as well as liquids, oxides and metals [12]. The elimination process of the sacrifice phase to obtain porosity can be performed by gradually increasing the temperature or through decomposition reactions [12–14]. As examples of the sacrificed components, the following can be quoted: wax [15], carbon black [16], sawdust and starch [17]. The possibility to control the structural characteristics of the final ceramic bodies is the main advantage of this technique. This method enables the production of bodies with porosity ranges between 20% and 90% and porous sizes between 1 and 700 μm [12,18].

In this work, eucalyptus sawdust was used as a sacrificial material and former of porosity. The entire forest in Brazil, with different species of trees, occupies an area of 7.83 million ha and is intended for the most varied uses. Of this entire forest, 73% (5.7 million ha) are occupied by planting eucalyptus trees, located mainly in the states of Minas Gerais (where this research was developed), São Paulo and Mato Grosso do Sul. An interesting characteristic of the eucalyptus plant is that there is regrowth. That is, after the first cut, there is a new plant sprouting on the stump (strain) that remained in the soil. The regrowth enables two more cuts.

Eucalyptus sawdust is produced concurrently with the processing of eucalyptus tree. Thus, there is no cost associated with its production. In addition, the eucalyptus sawdust is a non-toxic product, easily handled and easy to access in Brazil. It can be used without any previous treatment and it can be easily eliminated during the process of porous formation in the ceramic pieces, acting as a sacrifice phase.

The novelty of this work was to produce porous ZnO pieces using the sacrifice phase or the sacrificial fugitive technique as a conformation process. This technique and the eucalyptus sawdust were never applied to obtain porous pieces to be used in photocatalytic processes. There are no related cases of using the technique and raw material in the literature for water depollution. To aim this goal, the best conditions to obtain porous ceramic bodies obtained by uniaxial pressing with sacrifice phase were investigated in a way that it reaches high exposal area of the unwanted organic compounds to the oxidative sites in the photocatalytic processes using Rhodamine B (RhB) solution to perform the photocatalytic assays. Besides, the efficiency of the photocatalysts and its reuse was evaluated by the photocatalytic degradation of RhB, and a correlation between density, porosity and microstructural characteristics with the photocatalytic activity of the pieces was established using statistical data analysis.

Table 1
Green density of samples prepared by pressing with sacrifice phase

Sacrifice phase	Content (%)	Green density (g cm^{-3})
Eucalyptus sawdust	20	0.553 ± 0.0025
	25	0.451 ± 0.0017
	30	0.381 ± 0.0012

2. Materials and methods

This study was carried out based on the following stages: evaluation of physicochemical features of the starting materials; conditions used for obtainment of ZnO pieces; evaluation of physicochemical features of the pieces obtained and photocatalytic assays for Rhodamine B (RhB) discoloration.

2.1. Raw materials characterization

Initially, the raw materials zinc oxide powder (ZnO, 99% purity, Synth®, Av. Dr. Ulysses Guimarães, 3857 - Vila Nogueira, CEP: 09990-080 – Diadema/SP – Brazil) and eucalyptus sawdust were characterized by the X-ray diffraction technique, differential scanning calorimetry (DSC) and thermogravimetric analysis (TGA).

The X-ray diffraction technique was used in the structural characterization to determine the presented crystalline phases of the ZnO powder (JCPDS card N°. 36-1451). The tests were performed in a Rigaku® (Alfenas/MG, Brazil) Ultima IV (Cu Kα 0.1542 nm) equipment with analysis carried between 15° and 75° at 40 kV and 30 mA. The peaks were indexed to their respective crystalline planes using the Powder Cell 2.0 software.

DSC and TGA were used to determine the degradation temperature of the eucalyptus sawdust, which was used as a sacrifice phase, and to determine the best temperature of heat treatment of the samples containing the mixture of ZnO and eucalyptus sawdust. In both techniques (DSC and TGA), 10 mg of the material was added in platinum and rhodium alloy crucibles, in a Netzsch Jupiter STA 449F3 device, under a nitrogen atmosphere, with a heating rate of 10 K/min at a temperature range from 25°C to 800°C.

2.2. Processing

After the characterization of the precursor materials, pieces were prepared from a mixture of zinc oxide commercial powder (ZnO, 99% purity, Synth®, Av. Dr. Ulysses Guimarães, 3857 - Vila Nogueira, CEP: 09990-080 – Diadema/SP – Brazil) and eucalyptus sawdust (ES). In order to investigate the best ZnO:ES ratio that provides porous pieces with high mechanical strength, three variables were investigated during the processing of the samples. They are ZnO:ES proportion of precursors, applied pressure in the forming of the pieces and temperature of the thermal treatment of the pieces.

The composition of the ZnO:ES was varied in 80:20, 75:25% and 70:30%, in weight percentages. These components were weighed separately with an analytical scale, in order to prepare sample bodies with a final mass of 3 g. Organic binder carboxymethylcellulose (CMC, Graintec®, Avenida Brasil, 5133 - Distrito Industrial, 13505-600 Rio Claro/SP - Brazil) and water in the mass proportion of 5% and 10%, respectively, were used to assist in the sample pressing process.

After weighing, each composition investigated of the ZnO:ES, CMC binder and water were mixed and passed through a 1.40 mm sieve three times (to improve the homogeneity of the mixture), packed in plastic bags, closed and left to 24 h rest, aiming better homogeneity. Subsequently, the mixtures were pressed using a Marcon MPH-10 uniaxial hydraulic press, and a cylindrical steel mold with dimensions of 60.05 ± 0.01 mm (outer diameter) and 20.04 ± 0.01 mm (inner diameter). Two pressures were used to produce the pieces: 60 and 90 MPa.

Thirty-six samples were produced and distributed within two groups of 18 samples each. In the first group, the three different compositions of the ZnO:ES (80:20, 75:25 and 70:30) were pressed at 60 MPa, with six pieces produced for each composition. For the second group, the same three different compositions were pressed at 90 MPa, also with six pieces produced for each composition.

Before the sintering of the pieces, the green density (GD) of each sample was calculated using Eq. (1) below [19]:

$$\mathrm{GD}\left(\frac{\mathrm{g}}{\mathrm{cm}^3}\right)=\frac{1}{\left(X_a/\rho_a+X_b/\rho_b\right)} \tag{1}$$

where X_a and X_b are related to the mass fraction of the ES (sacrifice phase) and the ceramic material; ρ_a and ρ_b are associated to the densities, in this same order.

The samples were heat treated in a muffle furnace (EDG 3000), with a heating rate of 1°C/min. The heat treatment was carried out at temperatures of 800°C and 1,000°C for samples pressed at 60 MPa and at 90 MPa with a 2 h threshold time. At the end of the process, the samples produced were left to cool inside the furnace at a rate of 1°C/min until reaching room temperature.

2.3. Characterization of the pieces

Apparent specific mass (ASM) and apparent porosity (AP) were determined after the sintering (as given in Eqs. (2) and (3)) [9,20].

$$\mathrm{ASM}\left(\mathrm{g/cm^3}\right)=\left(\frac{P_{\mathrm{sat}}}{P_{\mathrm{sat}}-P_i}\right)\times\rho_{\mathrm{H_2O}} \tag{2}$$

$$\mathrm{AP}\left(\%\right)=\left(\frac{P_{\mathrm{sat}}-P_s}{P_{\mathrm{sat}}-P_i}\right)\times 100 \tag{3}$$

where P_s is the dry mass of the heat-treated samples, before they were put in water; P_i is the immersed mass; P_{sat} is the moist mass and $\rho_{\mathrm{H_2O}}$ is the water density.

DSC and TGA were used to evaluate endo/exothermic physico-chemical events and the mass variation of the composition containing the porous forming agent (eucalyptus sawdust). The conditions used were the same as previously described. Since the raw materials did not change, the analysis was performed only for the 75:25% of ZnO:ES sample without heat treatment.

Microstructural analysis (i.e., scanning electron microscopy [SEM]) and energy dispersive X-ray spectroscopy (EDS) – a chemical microanalysis technique used in conjunction with SEM – were performed using scanning electron microscopy Magellan 400 L equipment for the samples pressed at 90 MPa and heat treated at 800°C and 1,000°C with (a) 20%; (b) 25% and (c) 30% eucalyptus sawdust and the images were processed using the Image J software.

2.4. Photocatalytic performance

Rhodamine B (RhB) P.A. (Synth) was used as probe dye for the photocatalytic assays. These tests were conducted in a photochemical reactor operated under UV-C irradiation, with four Mercury vapor lamps (Philips® Ultraviolet G15T8 15 W, Philips do Brasil, Av. Marcos Penteado de Ulhoa Rodrigues, 939, Barueri – SP/Brazil) and a cooling system using circulating water in a copper serpentine through a thermostatic bath (Solab® SL152/18, Rua Luiz Silveira Pedreira, Piracicaba, SP/Brazil) at a temperature of 10°C. For the tests, 50 mL beakers were used, in which 15 mL of RhB (5 mg L^{-1}) was added, as well as the ZnO pieces. This analysis was also made only with the RhB solution, in order to compare the photocatalytic activity (blank). The system was maintained without irradiation and at room temperature for 1 h to assess the effects of adsorption. After exposure to UV-C irradiation inside the reactor for 2 h, regular interruptions every 15 min were made to obtain a chemical analysis of the photodegradation. Absorption spectroscopy in UV-Vis (Agilent Technologies Cary 60 UV-Vis, Av. Marcos Penteado de Ulhoa Rodrigues, 939, 6 andar, Castelo Branco Office Park, Torre Jacarandá. Tamboré, Barueri - SP 06460-040, 0800 7281405) was used to evaluate the difference in dye absorbance. The scan was performed in the 400–800 nm range, checking the absorbance spectra by referencing the wavelength with greater absorption for RhB (554 nm). All analyses were performed in triplicate.

In addition to the individual tests, a study of the reuse of the samples was performed. It was established five cycles of photodegradation in the same mode as the photocatalytic tests, so that at the end of each cycle, the selected samples were weighted, dried at room temperature over 24 h and, again submitted to the photocatalytic test.

Finally, using the T hypothesis, with a significance level of 0.05, applied using the Excel software (Microsoft®), the effect of the sintering temperature was evaluated in relation to the average porosity and photocatalytic activities for each content of the sacrifice phase studied and for each load applied. Through analysis of variance, with the same level of significance, using Sisvar [21], it was possible to compare the average properties analyzed with the percentages of the sacrifice phase used in the studied heat treated and pressing conditions.

3. Results and discussion

X-ray diffractometry was performed in order to analyze the crystalline structure of ZnO powder. This powder presented hexagonal crystalline structure (Fig. 1), corresponding to the zincite or wurtzite mineral (JCPDS card N°. 36-1451).

The relationship between loss mass and temperature changes for the eucalyptus sawdust was determined by DSC/TG analysis (Fig. 2). It is possible to observe endothermic events near the temperature of 100°C. This first peak is associated to the water disposal from the sample. There is also a higher peak from 300°C to 400°C. This second peak presents a larger mass variation and, considering the temperature range, it indicates that the complete decomposition of the eucalyptus sawdust occurs. The heat release shown in the DSC curve indicates the total thermal degradation of the eucalyptus sawdust.

In order to calculate the theoretical GD of the compositions containing ZnO and the eucalyptus sawdust, shown in Table 1, the value of 0.12 ± 0.001 g cm^{-3} was adopted for the sawdust density. This calculation was performed using the rule of mixtures (Eq. (1)). It was possible to observe that the highest GD was reached for the 20% in weight eucalyptus sawdust sample. Although it was the highest calculated value, it corresponds to approximately 10% of the theoretical density of the ZnO. Given that the correlation used to calculate the theoretical GD of the samples consider the content of each material and the respective density, the major values refer to the samples with higher contents of ZnO, since the oxide has the higher mass to volume ratio. Since the density of eucalyptus sawdust is lower, samples with a higher content of the sacrifice phase have lower porosities, as expected.

Given that the porous precursor (eucalyptus sawdust) could present a different characteristic when in contact with ZnO, a new thermal analysis was conducted for the pressed samples (green samples). Fig. 3 presents the evaluation made for a pressed sample at 90 MPa with 25% in weight of eucalyptus sawdust and ZnO. The analysis confirmed that the elimination of the organic material incorporated followed the same temperature range found in the thermal evaluation for the insulated material (Fig. 2). No further events were identified by the analysis.

Fig. 4 shows the values obtained for the apparent porosity for the ZnO samples pressed at 60 and 90 MPa with different contents of eucalyptus sawdust, heat treated at 800°C and 1,000°C. In general, it is possible to notice that the evaluated process established, in all cases, produced porous ceramic bodies with a minimum porosity of approximately 50% of the theoretical ZnO value. It was also observed that in all compositions, the different pressures applied did not result in significant changes to the evaluated properties.

On the other hand, when evaluating the system behavior considering the temperature effect, it is possible to notice that the samples heat treated at 1,000°C showed a higher porosity (Fig. 4) for all investigated compositions. The composition of 25% in weight of eucalyptus sawdust presented higher indexes of porosity for the samples. It is also possible to observe that, for different percentages of eucalyptus sawdust, above 30% or below 20% in weight of the content mentioned, the values of the porosity were reduced. This was even more evident when the analysis was focused only on sintering performed at 1,000°C. The tests performed have indicated that the content of sacrifice material and the obtained porosity were not directly proportional because other factors related to processing (heat treatment, conditions of pressing, additives presence) may have affected the obtained results.

With a fine granulometry, the material resulted in good homogenization conditions and, possibly, interconnected porosity in the bodies, which led to a better elimination of the sacrifice phase during the heat treatment. These observations are useful in understanding the reasons of why the higher temperature used in the heat treatment produced samples with higher porosity. At higher temperatures, the bodies possibly presented greater magnitude in the structural modification, favoring the interconnectivity of the pores and, thus, the elimination of organic compounds, increasing the porosity.

As stated in the ASM assessment, it was not possible to observe significant changes regarding the variation on the applied load and on the heat treatment temperature.

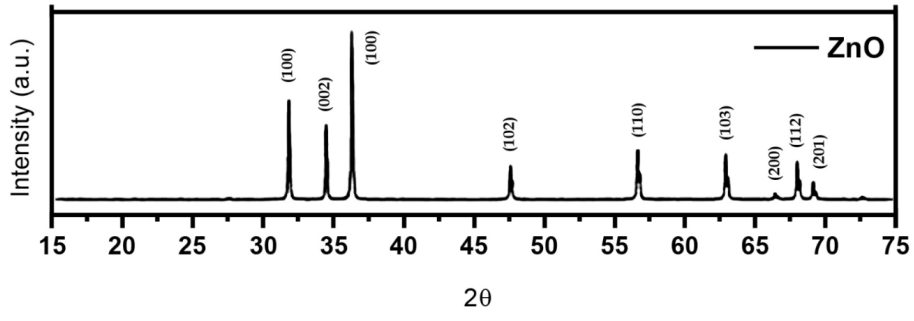

Fig. 1. X-ray diffraction of ZnO powder.

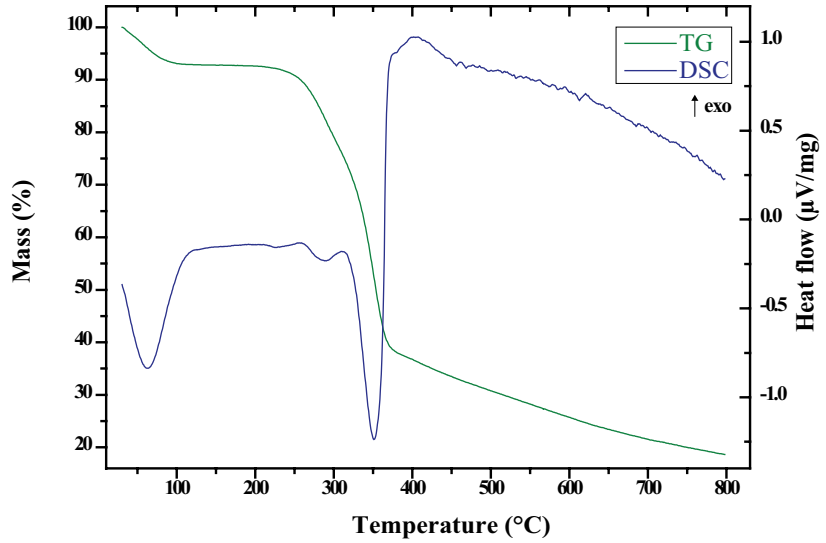

Fig. 2. Differential scanning calorimetry/thermogravimetric analysis for eucalyptus sawdust.

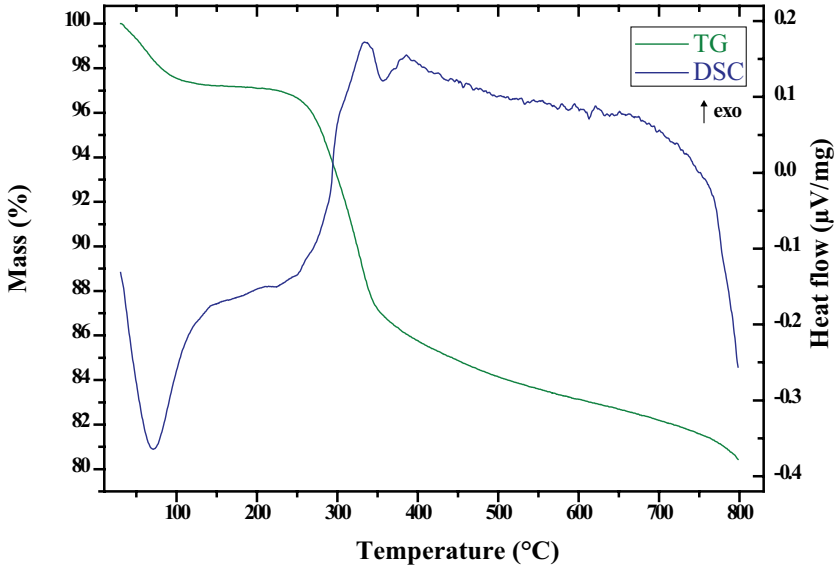

Fig. 3. Differential scanning calorimetry/thermogravimetric analysis for a 25% eucalyptus sawdust sample.

The ASM values for samples pressed at 60 and 90 MPa and heat treated at 800°C (varying from 2.44 to 2.70 g/cm^3) are similar to the samples heat treated at 1,000°C (varying from 2.39 to 2.60 g/cm^3).

Since there were no significant changes on porosity due to changes in the compaction load, the samples pressed at 90 MPa were selected to undergo microstructural analysis by SEM with EDS.

Fig. 5 shows the images of SEM for the samples heat treated at 800°C. The micrographs corroborate the results of apparent porosity indicating a higher level of porosity presented by the dark regions, related to the absence of zinc oxide (pores). The 25% in weight of eucalyptus sawdust composition shows a higher homogeneity in the porosity distribution. Contrary to what was analyzed in the compositions of the extremes, the 25% in weight of eucalyptus sawdust composition does not point to regions with excessive absence or agglomerates of zinc oxide particles, which thus indicates a homogeneously distributed porosity.

Fig. 6 shows the images of electron microscopy of the samples heat treated at 1,000°C. In all the discussed cases, the increase in temperature led to structural changes in the samples that basically summarize the densification due to particle size growth. In addition to presenting larger grains, the images also confirm the larger packaging for samples submitted to a higher content of eucalyptus sawdust. As the sintering time was the same for all samples, those with a reduced amount of ZnO content started the sintering process faster. The effects that characterize the beginning of the sintering process, mentioned above, can be seen in Fig. 6c.

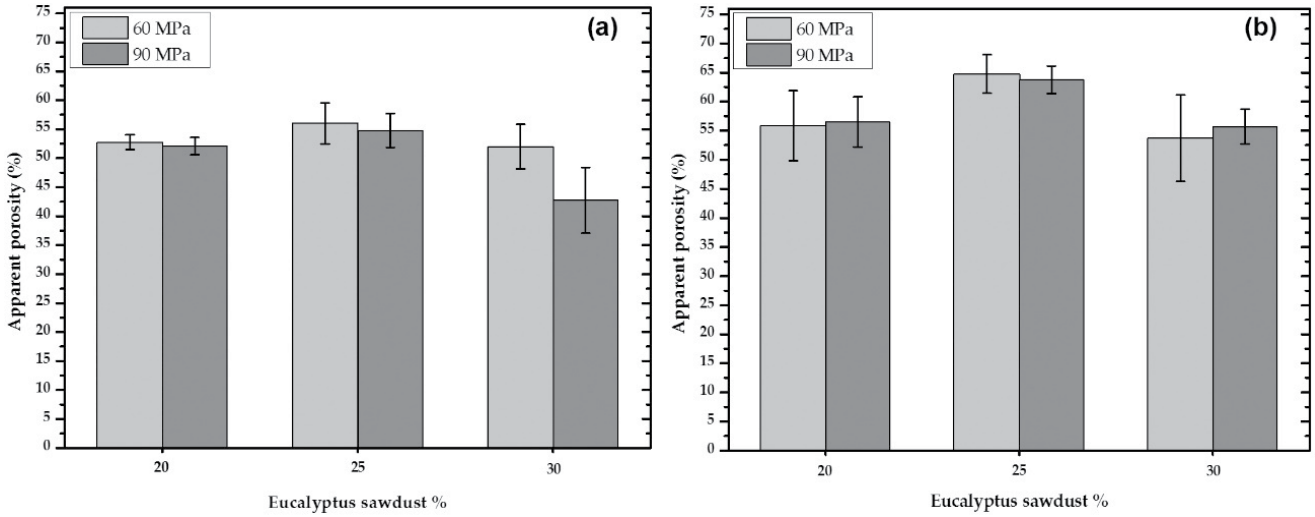

Fig. 4. Porosity values for sacrifice phase samples heat treated at (a) 800°C and (b) 1,000°C.

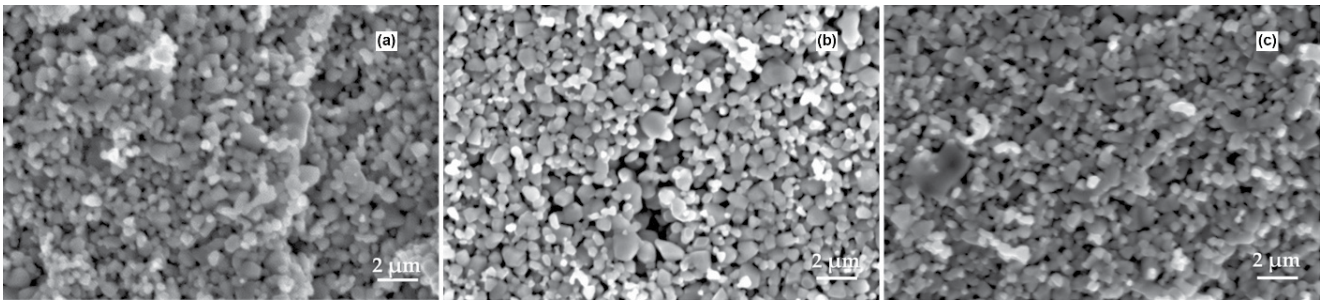

Fig. 5. Scanning electron microscopy of samples heat treated at 800°C with (a) 20%, (b) 25%, and (c) 30% eucalyptus sawdust.

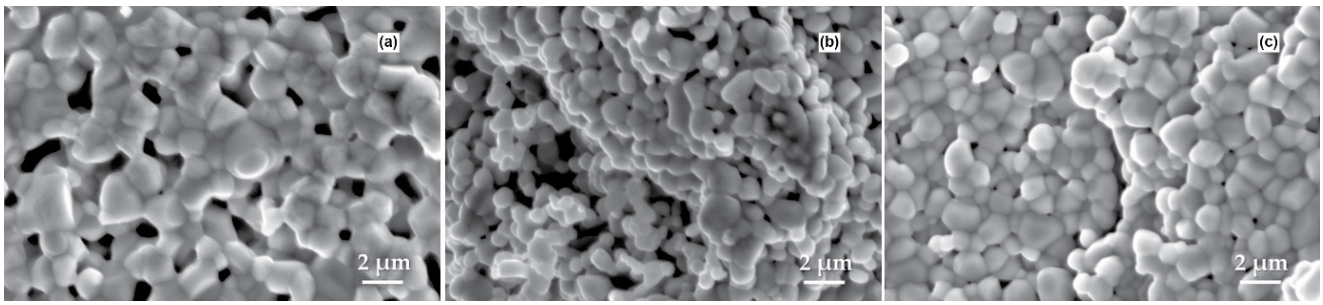

Fig. 6. Scanning electron microscopy of samples heat treated at 1,000°C with (a) 20%, (b) 25% and (c) 30% eucalyptus sawdust.

On the other hand, in Fig. 6b, larger regions associated with porosity can be found, justifying the higher porosity to the samples heat treated at 1,000°C with 25% in weight eucalyptus sawdust. Thus, the interconnectivity presented in the microstructures in Fig. 6 justify the higher values of porosity achieved for the treatment in question, as observed in Fig. 4.

The photocatalytic properties of the pieces were evaluated by the degradation of the RhB on the photocatalytic tests. In general, higher porosity samples and smaller grain sizes promote higher levels of dye degradation, indicating that photocatalytic properties are strongly influenced by microstructural aspects.

Fig. 5 indicates that the medium grain size (obtained by Image J software) of the samples heat treated at 800°C is approximately 0.5 micron while for samples heat treated at 1,000°C it is observed that the medium grain size is higher (1.8 microns). So, the smaller grain size of samples heat treated at 800°C may also have contributed to the best levels of dye degradation.

Fig. 7 shows the graphical relations that allow analyzing the discoloration of the dye.

All the samples presented high percentages of degradation, as shown in Table 2. However, the decrease in the RhB concentration was more expressive in reactions with samples obtained in 800°C.

Table 2
Levels of degradation* of samples obtained by uniaxial pressing with sacrifice phase

Composition (% of eucalyptus sawdust)	Compaction load applied (MPa)	Degradation % (800°C samples)	Degradation % (1,000°C samples)
20	60	57.97	45.07
	90	59.40	44.11
25	60	71.20	46.98
	90	79.36	46.01
30	60	75.16	50.72
	90	75.95	37.05

*Standard deviation of degradation for samples heat treated at 800°C had a range from 0.7% to 6.85%; samples heat treated at 1,000°C had a range from 1.52% to 3.17%.

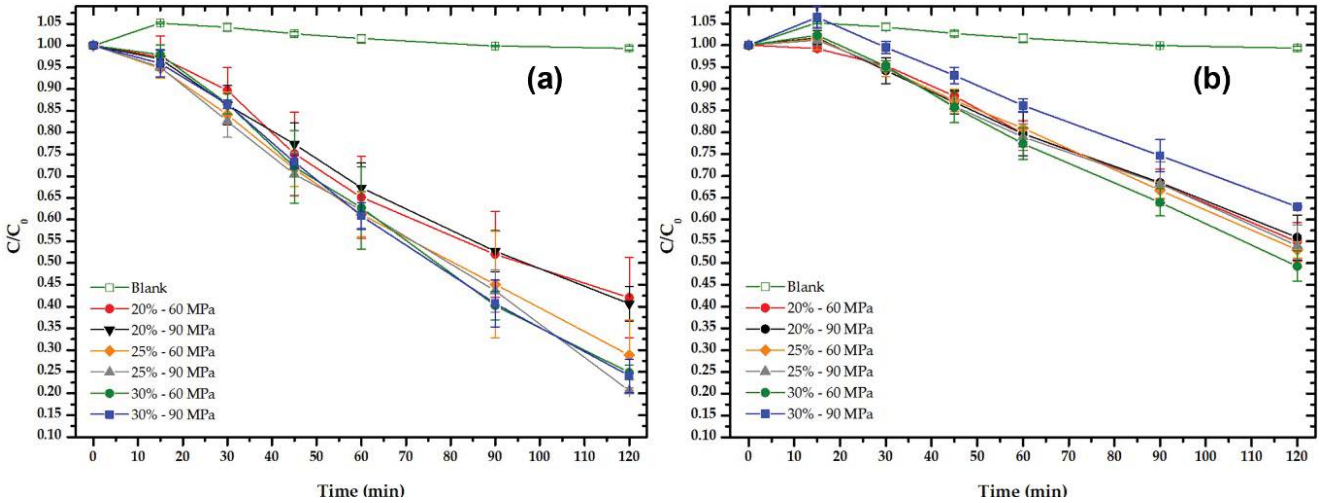

Fig. 7. Photocatalytic tests for the sacrifice phase samples heat treated at (a) 800°C and (b) 1,000°C.

In all investigated conditions, the degradation percentages did not vary considerably due to the porosity related to the compaction load. It is likely that the difference between the pressing values is not large enough to cause much difference in the final microstructure of the samples. On the other hand, the values of the analysis from Table 2 confirm the discussions made based in Fig. 7, indicating a higher degradation effectiveness using samples heat treated at 800°C.

This may also be related to the levels of porosity found, as they often justify the behavior of photocatalytic systems. As previously mentioned, higher porosity systems lead to higher photodegradation values. On the other hand, it is important to point out that, for the photodegradation process to be effectively established, there must be a high area of exposure of the semiconductor to incident irradiation [22–24]. In this case, the samples heat treated at 800°C, with less interconnectivity, even though presenting reduced porosity values, resulted in a greater area of exposure to the dye, favoring the photocatalytic process. Therefore, the microstructural images collaborate with the better understanding of what was observed for the porosity obtained and the photocatalytic activity achieved.

Thus, the sample with 25% in weight of eucalyptus sawdust, heat treated at 800°C, presented a higher level of porosity, which consequently obtained the best photodegradation rates. As there were no changes in the studied properties related to the pressing loads, two samples with 25% in weight of eucalyptus sawdust pressed at 90 MPa underwent photodegradation cycles. Table 3 shows the percentage of dye degradation over five cycles of photocatalysis.

It was possible to observe that, after all the established cycles, the samples still showed considerable photocatalytic activity followed by small changes in mass, as can be seen in the results of Table 4. These observations indicate the possibility of reusing the samples, and that eventual synthesis residues, supposedly adsorbed on the semiconductor surface, do not affect the process efficiency. There was an increase in the percentage of degradation of the dye in relation to the first values presented, and this tendency to increase the percentage of degradation in the first three cycles had already been reported in previous analyzes with similar systems [3]. Ruellas et al. [3] obtained ZnO ceramic pellets by slip casting, also intended to be used in the photocatalytic discoloration of RhB. Although the porous samples were produced by a different process, after the photocatalytic cycles with degradations of up to 99.95%, superficial changes were observed in the samples, possibly due to the leaching process, since it was possible to evaluate the

decrease in average grain size by microstructural images [3]. The same was found for the samples presented in this work, corroborating the trend verified in Table 3.

The first statistical evaluations established by the Student's *t*-test state that, as previously assessed physically, the compaction pressing values did not bring significant changes in the average porosity and in the photocatalytic activity. Both in heat treatments and in the evaluation of the influence of the applied pressing load, the results for the properties discussed were statistically equal. On the other hand, the statistical instrument points to an influence of the temperature on the porosity of the samples produced with 25% eucalyptus sawdust, pressed with 60 MPa. In this case, the average porosity, considering the variation in the heat treatment temperature, cannot be assumed to be statistically similar. In other conditions, where the effect of the temperature on porosity and photocatalytic activity was also evaluated, statistical similarities between the averages were studied. As previously presented, microscopic images helped in this evaluation and brought a clearer view of the changes observed in the experiments.

In addition, using the variance analysis with the same level of significance, it was possible to investigate the relation between the content of the sacrifice phase with porosity and photocatalysis at each temperature and compaction pressure used. In this case, in both heat treatments used, the samples identified with 25% eucalyptus sawdust presented a distinct statistical behavior for porosity when compared with the other compositions. Although the analysis indicates a statistical similarity for photocatalytic activity, the evaluations corroborate what was already observed regarding the physical and microstructural characterizations.

In the literature, ZnO is indicated as highly efficient when applied in photocatalytic decontamination processes. However, when used in particulate form, new treatment steps for the removal of zinc oxide after photocatalysis are necessary [4,23,24]. Trying to solve this problem, and to bring an alternative facilitated treatment of effluents with dyes using zinc oxide, other works explored the conformation of the material in porous ceramic parts. In this case, it is important to reconsider that porosity is one of the most important parameters, as it is associated with the surface of exposure to compounds that must be degraded.

Previous research indicates that pieces with lower porosity indexes were obtained when compared with the results presented here [3,24]. It is worth mentioning that different means of conformation were used.

Assuming that our experiment occurred in an equilibrium state, the active sites concentration can be considered constant and the recombination happened approximately at a constant rate. The light source during the experiments was constant too, so the average number of active sites is expected to be proportional to the surface area, which, for these experiments, is the only variable that could actively affect the active sites concentration. Since the present work has achieved results that associates high porosity with considerable levels of photodegradation, as well as in other similar works [3,24], it is accepted that the chosen processing technique can be pointed out as one of the best conformation method for the evaluated material, within the variables investigated here. In future perspectives, it is permissible to assume that pressing with sacrifice phase may be considered as one of the main methods to meet needs similar to the ones studied in this article.

Table 3
Degradation established in five photocatalysis cycles performed in samples with 25% eucalyptus sawdust, pressed at 90 MPa and heat treated at 800°C

Cycle	Level of degradation obtained (%)
1	76.55 ± 3.02
2	76.30 ± 2.76
3	79.45 ± 5.38
4	74.41 ± 4.28
5	74.79 ± 2.12

Table 4
Obtained masses of the samples after each photocatalytic cycle

Cycle	Sample 1 (g)	Sample 2 (g)
1	1.992	1.986
2	1.808	1.760
3	1.737	1.685
4	1.680	1.539
5	1.592	1.495
Initial mass	2.056	2.040

The ease of including porosity during processing, as well as the simple preparation of precursors, reinforce the choice of this technique. It is necessary to consider that the size and shape of the ceramics obtained are conditioned to the chosen mold. It is worth mentioning that the porosity achieved was higher than that of similar works [3,24] and the percentage of degradation of the ceramic samples of this work was satisfactory. Further studies varying other parameters such as different sacrifice materials and different organic binders can be investigated to optimize the photodegradation using the technique presented.

Thus, in general, this work presented a simple conformation technique (using a low-cost material as a porosity former), which makes it possible to obtain efficient, reusable and easily removable ZnO-based materials for water depollution.

4. Conclusions

ZnO pieces obtained by the sacrifice phase technique were successfully used as catalysts for RhB dye photodegradation. The ASM values for samples pressed at 60 and 90 MPa and heat treated at 800°C (varying from 2.44 to 2.70 g/cm^3) were similar to the samples heat treated at 1,000°C (varying from 2.39 to 2.60 g/cm^3). All samples presented high porosity values after heat treatment (above 50%), which confirms the efficiency of the eucalyptus sawdust as a porosity former and the sacrifice phase technique in obtaining porous bodies with good mechanical properties. Experimental results and statistical analysis

showed that no significant variation was observed related to the different compaction loads used and that the increase in porosity positively influenced the degradation of the RhB dye. The photocatalysts presented high efficiency in the degradation of RhB, with easy removal of the medium and viability in the reuse of the same sample in five cycles of photocatalysis, with small changes in mass, without additional stages of separation of the pieces of the reaction medium.

Acknowledgments

The authors gratefully acknowledge the support of the Conselho Nacional de Desenvolvimento Científico e Tecnológico, the Universidade Estadual de São Paulo on the Rio Claro campus and the Universidade Federal de Alfenas (UNIFAL – MG). This work was supported by the Brazilian research funding programmes and agencies Conselho Nacional de Desenvolvimento Científico e Tecnológico under grant 444117/2014-8 and Empresa Brasileira de Pesquisa Agropecuária under grant SEG 01.14.03.001.01.00.

References

[1] O.F. Lopes, V.R. Mendonça, A. Umar, C.R. Oliveira, Alto Desempenho Fotocatalítico do $ZnSn(OH)_6$ na Degradação da Rodamine B, M.A. Martins, O.B.G. de Assis, C. Ribeiro, L.H.C. Mattoso, Eds., Workshop da Rede de Nanotecnologia Aplicada ao Agronegócio, 7, São Paulo, Brazil, 2013, Embrapa Instrumentação: São Carlos, Brazil, 2013, pp. 389–391. Available at: http://ainfo.cnptia.embrapa.br/digital/bitstream/item/88411/1/Proci-13.00084.pdf

[2] F.F. Brites, N.R.C. Machado, V.S. Santana, Effect of support on the photocatalytic degradation of textile effluents using Nb_2O_5 and ZnO: photocatalytic degradation of textile dye, Top. Catal., 54 (2011) 264–269, https://doi.org/10.1007/s11244-011-9657-2.

[3] T.M.O. Ruellas, L.O.O. Peçanha, G.H.S. Domingos, S.C. Maestrelli, T.R. Giraldi, Photodegradation of Rhodamine B catalyzed by ZnO pellets, Cerâmica, 65 (2019) 47–53.

[4] P. Gonçalves, R. Bertholdo, J.A. Dias, S.C. Maestrelli, T.R. Giraldi, Evaluation of the photocatalytic potential of TiO_2 and ZnO obtained by different wet chemical methods, Mater. Res., 20 (2017) 181–189.

[5] K.M. Lee, C.W. Lai, K.S. Ngai, J.C. Juan, Recent developments of zinc oxide based photocatalyst in water treatment technology: a review, Water Res., 88 (2015) 428–448.

[6] P.C.S. Bezerra, R.P. Cavalcante, A. Garcia, H. Wender, M.A.U. Martines, G.A. Casagrande, J. Giménez, P. Marco, S.C. Oliveira, A.M. Junior, Synthesis, characterization, and photocatalytic activity of pure and N-, B-, or Ag-doped TiO_2, J. Braz. Chem. Soc., 28 (2017) 1788–1802.

[7] A. Pipi, G. Byzynski, L. Ruotol, Photocatalytic activity and RNO dye degradation of Nitrogen-doped TiO_2 prepared by ionothermal synthesis, Mater. Res., 20 (2017) 628–638.

[8] S. Matsuzawa, C. Maneerat, Y. Hayata, T. Hirakawa, N. Negishi, T. Sano, Immobilization of TiO_2 nanoparticles on polymeric substrates by using electrostatic interaction in the aqueous phase, Appl. Catal. B, 83 (2008) 39–45.

[9] L.R.P. Araújo, R.P.S. Dutra, Obtaining and analysis of porous ceramic with the incorporation of organic products to the ceramic body, Cerâmica, 48 (2002) 223–230.

[10] P. Colombo, E. Bernardo, L. Biasetto, Novel microcellular ceramics from a silicone resin, J. Am. Ceram. Soc., 87 (2004) 152–154.

[11] D.M. Liu, Preparation and characterization of porous hydroxyapatite bioceramic via a slip-casting route, Ceram. Int., 28 (1998) 441–446.

[12] A.R. Studart, U.T. Gonzenbach, E. Tervoort, L.J. Gauckler, Processing routes to macroporous ceramics: a review, J. Am. Ceram. Soc., 89 (2006) 1771–1789.

[13] Z.Y. Deng, T. Fukasawa, M. Ando, G.J. Zhang, T. Ohji, Microstructure and mechanical properties of porous alumina ceramics fabricated by decomposition of aluminum hydroxide, J. Am. Ceram. Soc., 84 (2001) 2638–2644.

[14] M.V. Carlesso, R.O. Giacomelli, S. Günter, S. Kroll, K. Rezwan, D. Koch, S. Odenbach, Near-net-shaped porous ceramics for potential sound absorption applications at high temperatures, J. Am. Ceram. Soc., 96 (2013) 710–718.

[15] E. Gregorová, W. Pabst, Process control and optimized preparation of porous alumina ceramics by starch consolidation casting, J. Eur. Ceram. Soc., 31 (2011) 2073–2081.

[16] P. Colombo, Conventional and novel processing methods for cellular ceramics, Philos. Trans. R. Soc. A, 364 (2006) 109–124.

[17] D. Marrero-Lopez, D. Marreno-López, J.C. Ruiz-Morates, J. Peña-Martínez, J. Canales-Vázquez, P. Núnez, Preparation of thin layer materials with macroporous microstructure for SOFC applications, J. Solid State Chem., 181 (2008) 685–692.

[18] K. Prabhakaran, A. Melkeri, N.M. Gokhale, S.C. Sharma, Preparation of macroporous alumina ceramics using wheat particles as gelling and pore forming agent, Ceram. Int., 33 (2007) 77–81.

[19] I.W. Donald, Methods for improving the mechanical properties of oxide glasses, J. Mater. Sci., 24 (1989) 4177–4208.

[20] Brazilian Association of Technical Standards, NBR 9778: Hardened Cement Mortar and Concrete - Determination of Water Absorption by Immersion, Rio de Janeiro – Brazil, 1995, pp. 1–4

[21] D.F. Ferreira, SISVAR: a program for analysis and teaching of statistics, Symposium, 6 (2008) 36–41.

[22] S. Ye, M. Yan, X, Tan, J. Liang, G. Zheng, H. Wu, B. Song, C. Zhou, Y. Yang, H. Wang, Facile assembled biochar-based nanocomposite with improved graphitization for efficient photocatalytic activity driven by visible light, Appl. Catal. B, 250 (2019) 78–88.

[23] Ü. Özgur, Ya.I. Alivov, C. Liu, A. Teke, M.A. Reshchikov, S. Dogan, V. Avrutin, S.J. Cho, H. Morkoç, A comprehensive review of ZnO materials and devices, J. Appl. Phys., 98 (2005) 041301/1 - 041301/103.

[24] T.M.O. Ruellas, L.O.O. Peçanha, G.H.S. Domingos, C.R. Sciena, J.O.D. Malafatti, E.C. Paris, S.C. Maestrelli, T.R. Giraldi, Zinc oxide pieces obtained by pressing and slip casting: physical, structural and photocatalytic properties, Environ. Technol., (2019) 1479–487X (In press).